Frequency-Domain Streak Camera and Tomography for Ultrafast Imaging of Evolving and Channeled Plasma Accelerator Structures

Zhengyan Li, Rafal Zgadzaj, Xiaoming Wang, Stephen Reed, Peng Dong, and Michael C. Downer

Citation: AIP Conference Proceedings **1299**, 121 (2010); doi: 10.1063/1.3520297
View online: http://dx.doi.org/10.1063/1.3520297
View Table of Contents: http://scitation.aip.org/content/aip/proceeding/aipcp/1299?ver=pdfcov
Published by the AIP Publishing

Frequency-Domain Streak Camera and Tomography for Ultrafast Imaging of Evolving and Channeled Plasma Accelerator Structures

Zhengyan Li, Rafal Zgadzaj, Xiaoming Wang, Stephen Reed, Peng Dong, Michael C. Downer

Department of Physics, University of Texas at Austin, Austin, TX, USA, 78712

Abstract. We demonstrate a prototype Frequency Domain Streak Camera (FDSC) that can capture the picosecond time evolution of the plasma accelerator structure in a single shot. In our prototype Frequency-Domain Streak Camera, a probe pulse propagates obliquely to a sub-picosecond pump pulse that creates an evolving nonlinear index "bubble" in fused silica glass, supplementing a conventional Frequency Domain Holographic (FDH) probe-reference pair that co-propagates with the "bubble". Frequency Domain Tomography (FDT) generalizes Frequency-Domain Streak Camera by probing the "bubble" from multiple angles and reconstructing its morphology and evolution using algorithms similar to those used in medical CAT scans. Multiplexing methods (Temporal Multiplexing and Angular Multiplexing) improve data storage and processing capability, demonstrating a compact Frequency Domain Tomography system with a single spectrometer.

Keywords: Laser plasma acceleration, Frequency Domain Holography (FDH), Frequency Domain Streak Camera (FDSC), Frequency Domain Tomography (FDT), pulse multiplexing
PACS: 42.40.Kw, 42.30.Wb, 52.38.Kd

INTRODUCTION

Intense laser pulses or particle bunches propagating through plasma create complex micrometer-scale, luminal-velocity wakefields that are challenging to image in the laboratory, and thus are often known in detail only through intensive computer simulations. Accurate single-shot visualization can improve fundamental understanding of the generation and evolution of laser plasma wakefield structures, and improve the functioning of plasma-based accelerators. In 2006 Matlis et al. [1] captured "snapshots" of quasi-static linear laser plasma accelerator structures using Frequency Domain Holography (FDH) [2]. Frequency Domain Holography use a temporally stretched probe-reference (P–R) pulse pair that co-propagates with an intense pulse and the plasma structures it creates (see Fig.1a). The probe pulse (wavelength λ_{pr}) covers the whole "object", accumulating phase shift

$$\Delta\phi_{pr}(r,\zeta,z) = \frac{2\pi}{\lambda_{pr}}\int_0^L [1-\eta(r,\zeta,z)]dz \tag{1}$$

because of the pump-induced refractive index structure $\eta(r,\zeta,z)$ over distance L. Here r denotes transverse distance from the pump propagation axis, ζ longitudinal distance behind the pump. $\Delta\phi_{pr}$ is reconstructed by interfering the probe with a temporally advanced "reference" pulse in a spectrometer, and Fourier analyzing the resulting frequency-domain hologram [1, 2, 3]. In the strongly nonlinear "bubble" regime [4], however, which is important for producing nearly monoenergetic, low-emittance electron beams, the "bubble" structure evolves significantly [5], elongating at the beginning to trap electrons and contracting in the end to yield mono-energetic e-beam. The evolution history of the wakefield structure is critical to laser plasma accelerator functions and to the quality of electron beams. However, as shown in Eq. (1), $\Delta\phi_{pr}$ in Frequency Domain Holography averages the evolving, z-depending $\eta(r,\zeta,z)$. To recover lost information, it is necessary to generalize Frequency Domain Holography to a new visualization technique, which yields a movie of the "bubble" evolution history.

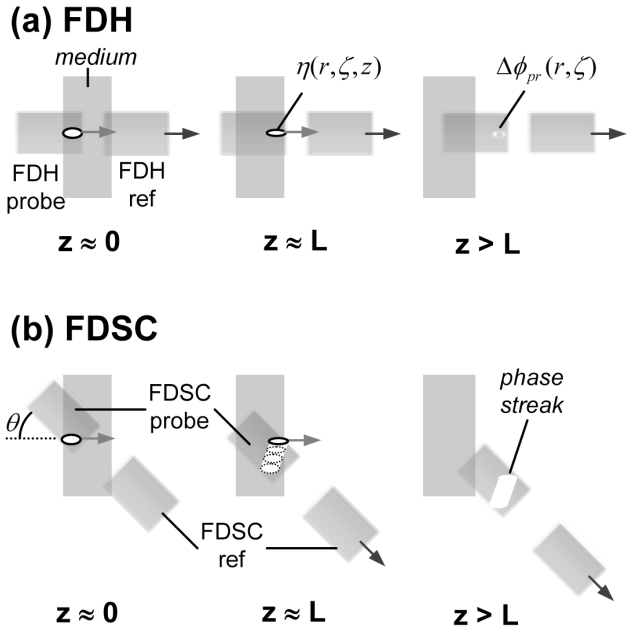

FIGURE 1. Schematic probe-reference (P–R) pulse configurations for **a.** Frequency Domain Holography (FDH) and **b.** Frequency Domain Streak Camera (FDSC) after pump has just entered ($z \approx 0$), is about to exit ($z \approx L$), and has exited ($z > L$) the medium. Arrows denote propagation directions of pump-induced index perturbation $\eta(r,\zeta,z)$ and chirped probe-reference pulses. The latter are imaged from $z = L$ to the entrance slit of a spectrometer.

FREQUENCY DOMAIN STREAK CAMERA

We generalize Frequency Domain Holography by including a Frequency Domain Streak Camera (FDSC), which uses a probe-reference pair that propagates at angle θ to the pump (see Fig. 1b). In the probe pulse frame, the evolving "bubble" sweeps across the probe profile with velocity

$$\vec{v} = \frac{v_p \cos\theta - v_{pr}}{1 - v_p v_{pr} \cos\theta/c^2}\hat{e}_{||} + \frac{v_p \sin\theta\sqrt{1 - v_{pr}^2/c^2}}{1 - v_p v_{pr}\cos\theta/c^2}\hat{e}_{\perp}, \tag{2}$$

imprinting a phase shift "streak" that records information about the bubble's evolution. Here $\hat{e}_{||}$ and $\hat{e}_{\perp}$ are parallel and perpendicular, respectively, to the probe propagation direction, while v_p and v_{pr} denote lab frame group velocities of pump and probe pulses, respectively, in the medium. The phase streak is reconstructed using conventional Frequency Domain Holography methods. A transverse line-out at a specific time of the streak perpendicular to its axis $\hat{v}$ accumulates phase shift as the bubble sweeps through. If the time interval taken by the bubble to sweep through the line-out is short enough compared to the whole propagation time that the bubble shape does not experience significant changes, the transverse line-out yields a projection of the bubble structure at the θ dependent projection angle

$$\phi(\theta) = \arctan\left(\frac{\sin\theta}{\cos\theta - v_{pr}/v_p}\right) - \theta, \tag{3}$$

with time resolution $d_{||}/v$, where $d_{||}$ is the bubble's dimension along $\hat{v}$. The Frequency Domain Streak Camera consisting of transverse line-outs at different time yields a time sequence of projections at the projection angle $\phi(\theta)$, revealing information about the bubble's evolution.

As a proof of concept, we performed a prototype experiment by creating an evolving bubble-like object by focusing a 600fs pump pulse (wavelength $\lambda_{pu} = 800$ nm, bandwidth $\Delta\nu = 30$ nm FWHM) inside a fused silica plate of thickness $L = 3$ mm. The pump induced refractive index $\eta(r,\zeta,z) = n_2 I(r,\zeta,z)$, where $n_2 \approx 3\times10^{-16}$ cm^2/W is the nonlinear index of glass and $I(r,\zeta,z)$ is the pump intensity profile. Thus $\eta(r,\zeta,z)$ evolves as the pump pulse diffracts, self-focuses, etc. Initial peak intensity I of the pump (focused here to spot radius $w_0 \sim 20$ μm at $z = 0$) varied between 0.04

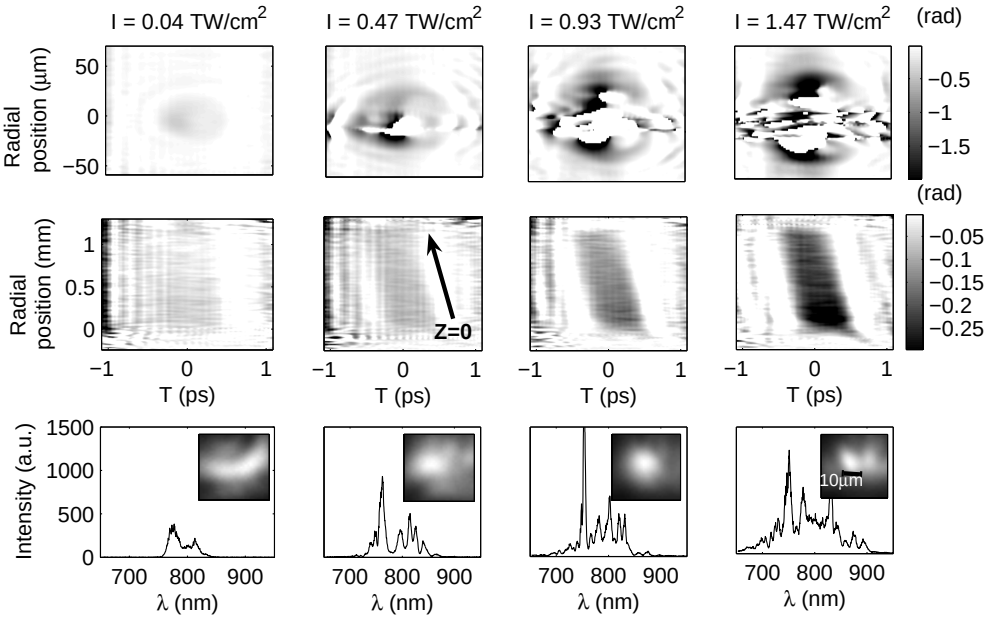

FIGURE 2. Phase shifts on 0° (top row) and 14° (middle row) probes, and transmitted pump spectrum (bottom row) and spatial profile (inset), for initial pump intensity (left to right) $I = 0.04,\ 0.47,\ 0.93,$ and 1.47 TW/cm^2.

and 1.5 (right) TW/cm^2 on different shots. In the upper end of this intensity range, $n_2 IL > \lambda_{pu}$, so pump propagation becomes nonlinear. Two linearly chirped, 1 ps, second harmonic ($\lambda_{pr} = 400$ nm) pulse pairs P1-R1 and P2-R2 probed $\eta(r,\zeta,z)$ simultaneously at $\theta = 0°$ (FDH) and 14° (FDSC), respectively. At 14°, the streak sweeps nearly transversely across the probe profile. The two pairs, each with probe and reference separated by $\Delta t_{PR} = 3.3$ ps, were imaged from the sample exit plane ($z = L$) of the silica plate to spatially offset locations at the spectrometer entrance slit so FDH and FDSC data were analyzed by a single spectrometer.

Figure 2 shows reconstructed images from the spatially multiplexed Frequency Domain Holography (top row) and Frequency Domain Streak Camera (2nd row) probes, and the spectrum (3rd row) and spatial profile (3rd row inset) of the pump at $z = L$ for four different I (indicated at top). The Frequency Domain Holography images show the longitudinally–averaged $\eta(r,\zeta,L)$. There are two complications in interpreting the Frequency Domain Holography images by themselves: (i) there is a discrepancy between the measured index "bubble" longitudinal extent ($\sim$1 ps) and the pump pulse duration ($\sim$600 fs) measured from a transverse line-out of the FDSC streak, which is caused by 450 fs group velocity walk-off between 800 nm pump and 400 nm probe; and (ii) phase wrapping artifacts created by $\Delta\phi_{pr}$ exceeding 2π near $r = 0$ appear at large I. These complications underscore the importance of Frequency Domain Streak Camera.

The Frequency Domain Streak Camera images (Fig.2, middle row) show a distinct phase streak that increases in amplitude with I. Line-outs along the streak axis, plotted in Fig.3(a), reveal intensity-dependent evolution of the axial phase shift. To help interpret this evolution, we modeled propagation of Gaussian pump pulses using the nonlinear Schrödinger equation, including multi-photon absorption and plasma formation [6]. Fig.3(b) shows the calculated peak pump intensity $I(z)$ for various initial I. For $I = 0.04$ TW/cm^2, nonlinearities are negligible, $I(z)$ decreases monotonically by linear diffraction over Rayleigh range $z_R = \pi n_0 w_0^2/\lambda_{pu} \approx L$, and the transmitted pump spectrum is barely perturbed from the incident spectrum (Fig.2, 3rd row, left). For $I = 0.47$ TW/cm^2, peak pump power (3 MW) reaches critical power $P_{cr} = \pi(0.61)^2\lambda_{pu}^2/8n_0n_2$ = 2.15 MW, and the pump propagates with nearly constant intensity, indicating a balance between self-focusing and diffraction with multi-photon absorption still weak. Simultaneously, we begin to observe pump frequency broadening to $\Delta\nu \sim 50$ nm (Fig. 2, 3rd row, 2nd panel), a signature of self-phase modulation. As pump intensity increases further ($I = 0.70$ to 1.47 TW/cm^2), nonlinear Schrödinger equation calculations show: (i) the pump self-focuses closer and closer to the glass entrance, initially increasing its intensity,

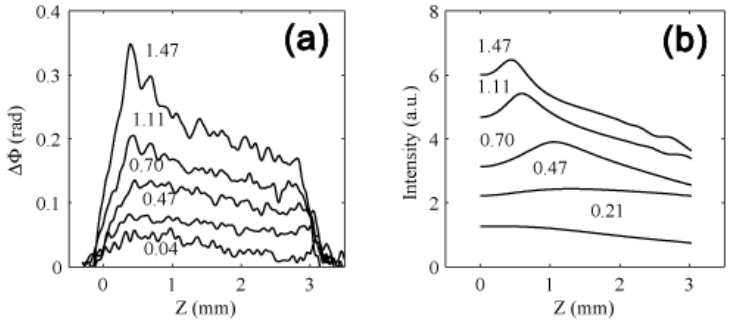

FIGURE 3. **a.** Measured line-outs along streak axis. **b.** Calculated line-outs along streak axis based on the generalized nonlinear Schrödinger equation.

followed by a monotonic decrease in intensity (see Fig. 3(b)); (ii) direct multi-photon absorption is the primary cause of the monotonic intensity decrease; (iii) the pump converges to a nearly intensity-independent transverse Townes profile [7] with FWHM 16 μm, in good agreement with the exit profiles shown in the insets of the last two panels, 3rd row of Fig. 2. Meanwhile the transmitted pump spectrum further broadens (Fig. 2, 3rd row, last 2 panels), indicating stronger self-phase-modulation. The transverse FWHM of the FDH phase profiles (Fig.2, top row) agree well the exit pump profiles and nonlinear Schrödinger equation calculations (their apparent broadening with increasing I results from increased visibility of the wings as total $\Delta\phi_{pr}$ increases). The initial self-focusing accounts for the large $\Delta\phi_{pr}$ near the center of the Frequency Domain Holography images at high I. The example illustrates how combining information from Frequency Domain Holography and Frequency Domain Steak Camera improves accuracy of interpretation.

PROBE MULTIPLEXING FOR FREQUENCY DOMAIN TOMOGRAPHY

Frequency Domain Tomography (FDT) with streak cameras at different θ corresponds to time sequences of projections at multiple projection angles ϕ. Projections at a specific time from each streak can be processed using tomographic algorithms [8] to reconstruct an instantaneous "frame" of the bubble's structure at that time. Repeating the procedure for different times yields a multi-frame "movie", all from single-shot data. If we assume that the pump laser pulse or particle beam is cylindrically symmetric so the bubble is symmetric as well, the projection angle $\phi(\theta)$ ranging from 0° to 90° can provide enough information to reconstruct bubble evolution without "streak artifacts" [9]. However, if the bubble is not perfectly cylindrically symmetric in reality and the required projection angle range is $\phi \in [0^\circ, 180^\circ]$, two color probe sets with wavelength larger and smaller than pump respectively are needed, in order to avoid too small phase shift on probes that counterpropagate with the pump ($\theta > 90^\circ$). 873 nm Stokes line generated by pumping Ti:Sapphire crystal with 800 nm laser pulse in chirped Raman pulse amplification (CRPA) [10] would be used as the other color of probes beside the already used frequency doubled 400 nm probes.

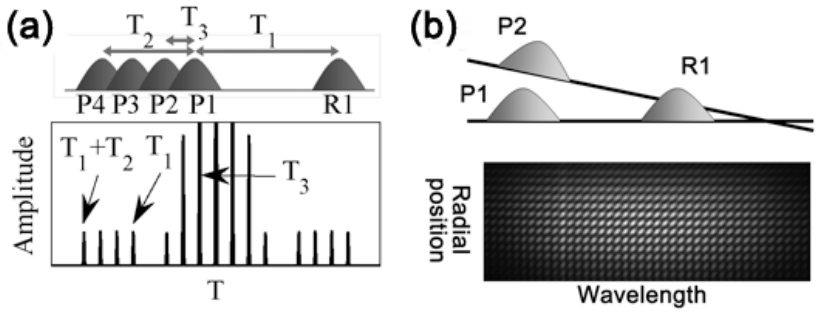

FIGURE 4. Probe pulses multiplexing. **a.** Temporal multiplexing pulse arrangement and Fourier transform of raw frequency domain hologram line-out; **b.** Angular multiplexing pulse arrangement and raw frequency domain hologram data.

Compact and cost-effective Frequency Domain Tomography is achieved by temporal multiplexing and angular multiplexing methods to collect probes at different θ with a single spectrometer in a single shot. In temporal multiplexing, one reference pulse and several probes are combined into a single pulse train as shown in Fig.4(a). The raw frequency-domain hologram shows multiple frequency domain modulations as a result of different time delays between pulses. A 1-D Fourier transform in frequency isolates peaks corresponding to interference between the reference and each probe. We have demonstrated 3-probe temporal multiplexing experimentally with probes separated by $\sim$ 400 fs to avoid overlap between neighboring peaks in the Fourier transform data, and thus to avoid cross-talk between different probes.

In angular multiplexing, several reference-probes sequences like the one in Fig.4(a) propagate into the spectrometer slit at slightly different angles, as shown in Fig.4(b), creating interference fringes along the transverse dimension of the hologram in addition to the conventional longitudinal frequency-domain fringes. The result is a 2-D grid-like map of interference fringes. A 2-D Fourier transform isolates peaks corresponding to probes at specific time delays behind the reference and specific angles of incidence into the spectrometer. We have experimentally demonstrated 3 probes at 0°, 0.6°, and 3° angles angularly multiplexed and 3.3 ps separated from the reference without cross-talk in reconstruction. These results demonstrate the feasibility of multiplexing tens of probes to a single spectrometer for compact, low-cost Frequency Domain Tomography.

CONCLUSION

We implemented Frequency Domain Holography with Frequency Domain Streak Camera to observe the evolution of a microscopic light-speed object, demonstrating the possibility of visualizing evolving wakefields in the nonlinear "bubble" regime. Moreover, Frequency Domain Streak Camera with probes at multiple angles yields Frequency Domain Tomography, which can reconstruct a time sequence of a quasi–static snapshots, like frames of movie, of evolving laser wakefields. By using temporal and angular multiplexing methods, we demonstrated a compact setup which is able to process data from multiple probes with a single spectrometer.

Oblique angle Frequency Domain Streak Camera and Frequency Domain Tomography can also find their application in situations where a collinear probe is not available. For example, in the generation of high quality electron beam above 1 GeV [11] and future Berkeley Lab Laser Accelerator (BELLA) experiments, a gas-filled capillary discharged plasma waveguide [12] is used, scrambling any wakefields structure encoded in the phase shift imprinted on a copropagating probe. However, the problems with conventional Frequency Domain Holography can be solved by having oblique angle Frequency Domain Tomography probes cross the waveguide area from windows on both sides. Thus Frequency Domain Tomography should enable laboratory visualization of channeled laser plasma accelerator structures for the first time. With Frequency Domain Streak Camera or Frequency Domain Tomography, we can expect a movie of "bubble" evolution for better understanding of laser–plasma interactions, and a compact instrument diagnosing laser plasma accelerator structures for 10 GeV electron generation in various applications.

ACKNOWLEDGMENTS

This work was supported by U.S. DoE grants DE-FG02-07ER54945 and DE-FG02-96ER40954 and NSF grant PHY-0936283.

REFERENCES

1. N. Matlis, S. Reed, S. S. Bulanov, V. Chvykov, G. Kalintchenko, T. Matsuoka, P. Rousseau, V. Yanovsky, A. Maksimchuk, S. Kalmykov, G. Shvets and M. C. Downer, *Nature Phys.* **2**, 749–753 (2006).
2. S. P. Le Blanc, E. W. Gaul, N. H. Matlis, A. Rundquist and M. C. Downer, *Opt. Lett.* **25**, 764–766 (2000).
3. J. P. Geindre, P. Audebert, A. Rousse, F. Falliès, J. C. Gauthier, A. Mysyrowicz, A. Dos Santos, G. Hamoniaux and A. Antonetti, *Opt. Lett.* **19**, 1997–1999 (1994).
4. A. Pukhov and J. Meyer-ter-Vehn, *Appl. Phys. B* **74**, 355 (2002).
5. S. Kalmykov, S. A. Yi, V. Khudik, G. Shvets, *Phys. Rev. Lett.* **109**, 135004 (2009).
6. A. L. Gaeta, *Phys. Rev. Lett.* **84**, 3582–3585 (2000).
7. K. D. Moll, A. L. Gaeta and G. Fibich, *Phys. Rev. Lett.* **90**, 203902 (2003).
8. A. C. Kak and M. Slaney, *Principles of Computerized Tomographic Imaging*, IEEE Press, New York, 1987.

9. H. Stark, *Image Recovery: Theory and Application*, Academic Press, New York, 1987, pp. 325.
10. F. Grigsby, P. Dong and M. C. Downer, *J. Opt. Soc. Am. B* **25**, 346–350 (2008).
11. W. P. Leemans, B. Nagler, A. J. Gonsalves, Cs. Tóth, K. Nakamura, C. G. R. Geddes, E. Esarey, C. B. Schroeder, and S. M. Hooker, *Nature Phys.* **2**, 696–699 (2006).
12. A. Butler, D. J. Spence, and S.M. Hooker, *Phys. Rev. Lett.* **89**, 185003 (2002).